



**Universiteit
Leiden**
The Netherlands

Water on well-defined platinum surfaces : an ultra high vacuum and electrochemical study

Niet, M.J.T.C. van der

Citation

Niet, M. J. T. C. van der. (2010, October 14). *Water on well-defined platinum surfaces : an ultra high vacuum and electrochemical study*. Retrieved from <https://hdl.handle.net/1887/16035>

Version: Corrected Publisher's Version

License: [Licence agreement concerning inclusion of doctoral thesis in the Institutional Repository of the University of Leiden](#)

Downloaded from: <https://hdl.handle.net/1887/16035>

Note: To cite this publication please use the final published version (if applicable).

Adaptability is not imitation. It means power of resistance and assimilation.

Mahatma Gandhi (1869–1948)

10

Impedance spectroscopy of H and OH adsorption on stepped single-crystal platinum electrodes in alkaline and acidic media

Abstract *The adsorption kinetics of hydrogen and hydroxyl on Pt(111) and stepped Pt[n(111) × (110)] electrodes with $n = 29, 9,$ and 4 in acidic and alkaline electrolytes have been studied using impedance spectroscopy. We found a potential dependent charge transfer resistance, R_{ct} , ($\sim 30 \Omega \text{ cm}^2$ to $\sim 1 \text{ k}\Omega \text{ cm}^2$) for hydrogen underpotential deposition in alkaline media (0.05 M NaOH), whereas in acidic media (0.025 M HClO_4) R_{ct} was too low to be determined accurately. Assuming simple (mean field) isotherms to fit our data, we obtain repulsive interactions between H_{upd} at the (111) terrace and effective attractive interactions at the steps. The adsorption of OH on (111) terraces is fast in both acidic and alkaline media.*

10.1 Introduction

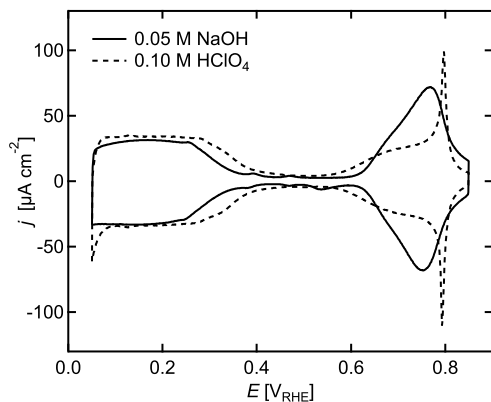


Figure 10.1 Cyclic voltammograms of Pt(111) in 0.10 M HClO_4 (dashed line) and 0.05 M NaOH (solid line), sweep rate 50 mV s^{-1} .

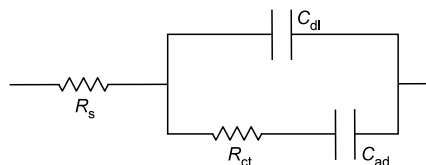


Figure 10.2 Equivalent circuit for H_{upd} .¹⁶⁹

The adsorption of hydrogen on platinum from aqueous solutions has been one of the main themes in surface electrochemistry for decades. In acidic media this reaction has been studied extensively, see for example.^{169–177} The underpotential deposition of hydrogen (H_{upd}) on Pt(111) occurs between 0.05 and 0.35 V. The evolution of H_2 takes place through the formation of overpotential deposited hydrogen at lower potentials (H_{opd}). In alkaline media, the cyclic voltammogram (CV) of Pt(111) in the 0.05–0.35 V region is comparable to the CV in acidic media, except for a small shift at high potential, as shown in figure 10.1. By comparing these CVs one would conclude that the H_{upd} is very similar in acidic and alkaline media. The region from 0.50 V (HClO_4) or 0.60 V (NaOH) to 0.85 V in the CVs is attributed to the adsorption of OH^{96} . The symmetry of the voltammogram suggests that the reaction is reversible, *i.e.* is very fast. A more suitable technique to study fast interfacial reactions is impedance spectroscopy, since this technique can measure processes at different time scales. For most systems with one adsorbate, like H_{upd} without other anions, the impedance response is modeled by the equivalent circuit shown in figure 10.2. In this circuit R_s is the resistance of the electrolyte, C_{dl} is the capacitance of the double layer, and R_{ct} (charge transfer resistance) and C_{ad} represent the kinetics of the adsorption.¹⁶⁹

Conway *et al.* have performed impedance spectroscopy measurements on H_{opd} and H_{upd} on Pt(111) and stepped Pt surfaces both in acidic and alkaline media. They showed that for acidic media (0.5 M H_2SO_4) the kinetics of H_{upd} on well-ordered Pt(100) and (311) are slower than on Pt(111) and (110) geometries and that

each geometry has a distinct double layer structure.^{98,169} Kolb *et al.* measured the C_{dl} of Pt(111)¹⁷⁴ and Pt(100)¹⁷⁸ in perchlorate solutions. Since the kinetics of the hydrogen adsorption in acidic media are too fast to be measured with common techniques (*i.e.* $R_{ct} = 0$), the circuit shown in figure 10.2 reduces to a simple RC circuit where no distinction can be made between the double layer capacitance and the adsorption capacitance. Therefore, they used very low HClO_4 concentrations (0.1 mM) in KClO_4 to separate the capacitances. They found a double layer capacitance of $\sim 20 \mu\text{F cm}^{-2}$ with a hump at $\sim 50 \mu\text{F cm}^{-2}$ around 0.43 V. They suggested this capacitance peak to be related to the potential of zero charge.

In alkaline media the kinetics of hydrogen adsorption are significantly slower. In this case the adsorption kinetics and the double layer capacitance can be separated. Oelgeklaus *et al.* measured the rate of hydrogen adsorption on platinum.⁹⁷ The rate of hydrogen adsorption appears to be one order of magnitude higher on Pt(111) than on polycrystalline Pt. In 1 M KOH they found that for hydrogen R_{ct} was $4 \Omega \text{ cm}^2$ at E 0.1 V, whereas for polycrystalline platinum it was $39 \Omega \text{ cm}^2$. Langkau and Baltruschat compared the rate of hydrogen adsorption on Pt(111) and Rh(111), and found that the rate of hydrogen adsorption in alkaline media on Rh(111) is smaller than on Pt(111) by two orders of magnitude.¹⁷⁹

Barber and Conway studied the H_{opd} region at various Pt single crystals in 0.5 M NaOH.⁹⁸ The rates of H_2 evolution are significantly slower in basic than in acidic media, due to the H atom being abstracted from H_2O instead of H_3O^+ . The order of reactivity for the different surface geometries is the same for acidic and alkaline media and was found to be $(100) < (111) < (110)$. For the H_{opd} at $E = -0.15 \text{ V}$ they found R_{ct} values of 2, 16, and $36 \Omega \text{ cm}^2$ for Pt(110), (111), and (100), respectively.

We report here the impedance of Pt(111) and stepped Pt[$n(111) \times (110)$] electrodes with $n = 29, 9$, and 4 in acidic and alkaline electrolytes for both H and OH adsorption. The adsorption kinetics of H and OH are compared for the different electrolytes and surface geometries and a model for the observed behavior will be suggested.

10.2 Experimental

All experiments were carried out in an electrochemical cell using a three-electrode assembly at room temperature. The cell and glassware were initially cleaned by boiling in a mixture of 1 : 1 concentrated sulfuric and nitric acid and before each experiment by boiling with ultra clean water (Millipore MilliQ gradient A10 system, $18.2 \text{ M}\Omega \text{ cm}$). A platinum wire was used as counter electrode and a reversible hydrogen electrode (RHE) in the same electrolyte was used as reference electrode. All potentials in this paper are referred to this electrode.

The experiments in acidic and alkaline media were carried out in, respectively,

0.025 M HClO₄ and 0.05 M NaOH prepared from high purity reagents (Merck 'Suprapur') and ultra clean water. The concentrations are chosen such that R_s is similar in both acidic and alkaline media. Argon (Linde, 6.0) bubbling was used to remove oxygen from the solution. The Ar was first bubbled through a 4 M KOH solution in order to remove carbonaceous impurities.

Bead-type Pt(111) and Pt[$n(111) \times (110)$] electrodes with $n = 29, 9,$ and 4 were used. Before each experiment the electrode was flame annealed for 30 s and cooled down to room temperature in an Ar + H₂ (Linde, 6.0) atmosphere. The electrode was transferred to the electrochemical cell with a protective droplet of deoxygenated water at the surface. All measurements were carried out with the Pt single crystal electrodes in a hanging meniscus configuration. Since impedance measurements take a relatively long time (10–15 min) we had to compromise between the optimal meniscus and its stability.

CVs and impedance spectra were collected using a computer controlled Ivium A06075 potentiostat. Impedance spectra were measured with frequencies from 10⁴ to 0.5 Hz and an amplitude of 5 mV. Equivalent circuits were fitted to the data with Ivium 1.420 software.

Blank CVs at a sweep rate of 50 mV s⁻¹ were recorded after each surface preparation in order to verify a clean and ordered state of the surface. After a series of impedance measurements, CVs were recorded again to ensure that no significant poisoning or surface changes had occurred during the time of data acquisition. In most cases, only one set of impedance measurements could be recorded with a fresh solution and an annealed crystal. Measuring more series gave rise to a reduced H_{upd} charge both at the terraces and the steps.

Sometimes a small peak at 0.55 V is seen in alkaline media in the reverse scan of the CV. This is due to contamination of the NaOH, which increases slightly over time. We measured the impedance at different levels of contamination and its magnitude did not have any influence on the impedance spectra. In KOH solution Oelgeklaus *et al.* observe the same feature. They did not observe any influence in the impedance spectra either.⁹⁷

Under these experimental conditions and using this data analysis we have measured the H_{upd} on Pt(100) in H₂SO₄ and found very good agreement with the data of Morin *et al.*,¹⁶⁹ indicating the validity of our methods.

10.3 Results

10.3.1 Pt(111)

Typical impedance spectra observed in the H_{upd} potential region (0.15 V) at Pt(111) in, respectively, acidic and alkaline media are shown in figure 10.3a and 10.3c. In figure 10.3a the absolute magnitude of the impedance, $|Z|$, is plotted versus fre-

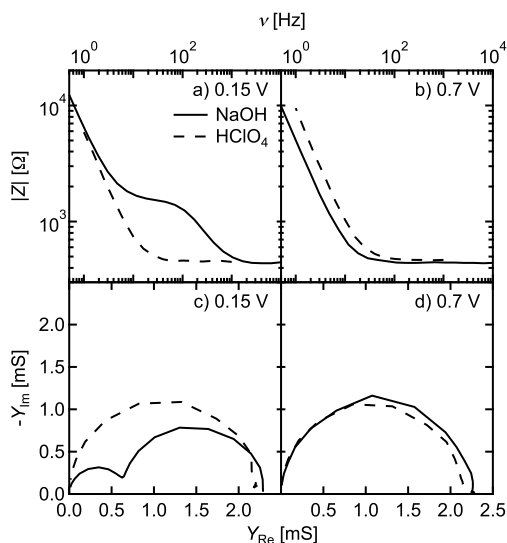


Figure 10.3 Bodeplots of Pt(111) in 0.05 M NaOH (solid line) and 0.025 M HClO₄ (dashed line) at a) 0.15 V and b) 0.7 V. c) and d) The corresponding admittance plots.

quency, ν . The dashed line shows the spectrum in acidic media, whereas the solid line shows the one in alkaline media. $|Z|$ increases from $\sim 100 \Omega$ for 10 kHz to $\sim 10 \text{ k}\Omega$ for 0.5 Hz both in acidic and alkaline media. In acidic media the increase of $|Z|$ starts at approximately 100 Hz. In alkaline media there is a second feature between $\sim 1 \text{ kHz}$ and $\sim 100 \text{ Hz}$. The corresponding admittance, Y , plots are shown in figure 10.3c. Here, the imaginary admittance is plotted versus the real admittance. In alkaline media the admittance plot shows two semi circles whereas only one semi circle is obtained in acidic media. The same spectra but in the OH adsorption region (0.70 V) are shown in figure 10.3b and 10.3d. Spectra in acidic media show similar behavior to the 0.15 V spectra. Remarkably, in this potential region no significant difference is observed between acidic and alkaline media.

We have measured impedance spectra at Pt(111) in the whole potential range of the CV shown in figure 10.1 with intervals of 50 mV. In HClO₄ the admittance spectra consistently show only one semi circle in the entire potential range (data not shown). For NaOH the admittance spectra up to 450 mV are shown in figure 10.4. In the H_{upd} potential range two semi circles are observed, with the semi circle at low frequencies becoming smaller with increasing potential. At potentials from 0.40 V and higher, only one semi circle is observed, comparable to HClO₄.

The equivalent circuit shown in figure 10.2 was fitted to the impedance data at each potential and the obtained values are plotted in figure 10.5 both for NaOH (10.5a) and HClO₄ (10.5b). The open circles represent R_{ct} and the squares and trian-

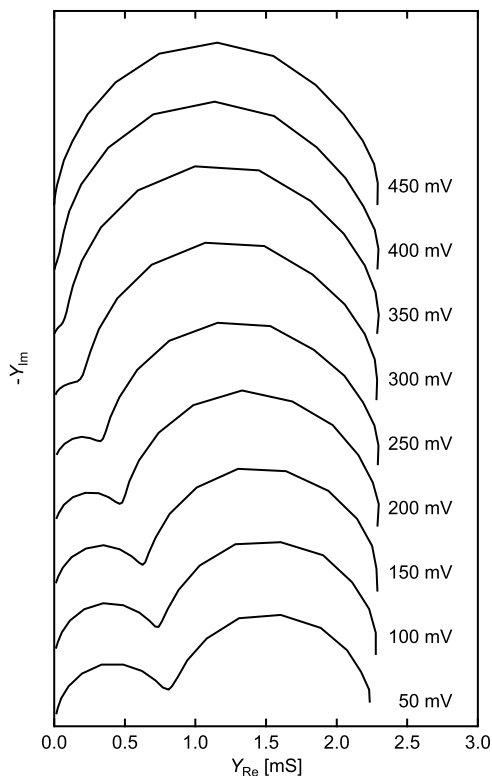


Figure 10.4 Admittance plots of Pt(111) in 0.05 M NaOH from 0.05–0.45 V.

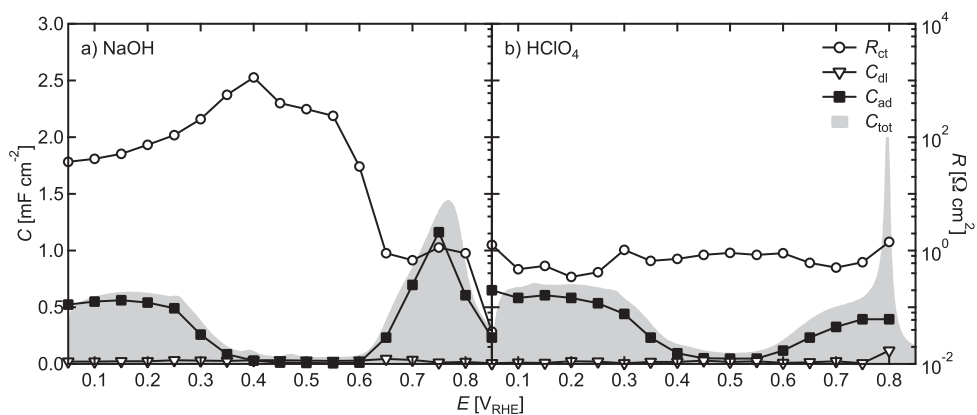


Figure 10.5 Fitted data of Pt(111) in (a) 0.05 M NaOH and (b) 0.10 M HClO₄. C_{tot} is calculated from the CV current.

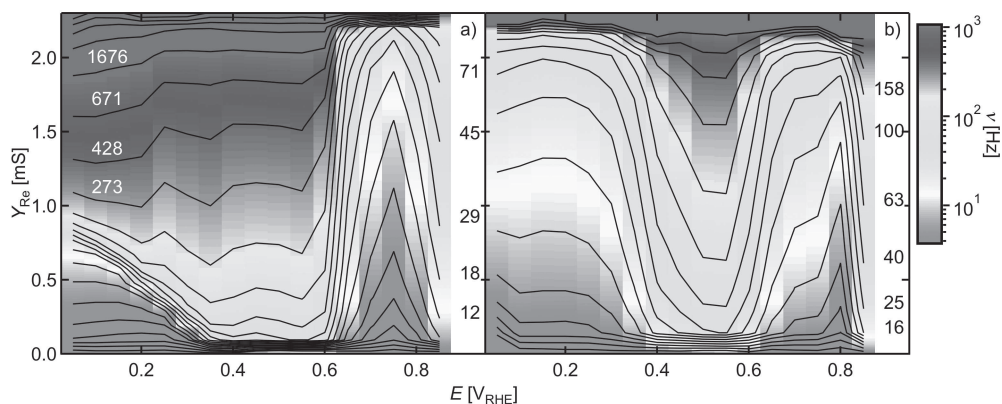


Figure 10.6 Frequency profile of the admittance plots of Pt(111) in (a) 0.05M NaOH and (b) 0.025 M HClO₄. The dashed lines connect the data points with the same frequency at different potentials.

gles represent C_{ad} and C_{dl} , respectively. The gray area shows the total capacitance C_{tot} which was calculated from the CV by

$$C_{tot} = \frac{j}{v_s} \quad (10.1)$$

where j is the current density obtained from the CV and v_s is the sweep rate, in this case 50 mV s^{-1} . C_{tot} is also equal to the sum of C_{ad} and C_{dl} . From figure 10.5 it is clear that C_{tot} is mainly determined by C_{ad} both in acidic and alkaline media. C_{dl} varies little between $10\text{--}30 \mu\text{F cm}^{-2}$. R_s is independent of the applied potential and is $\sim 400 \Omega$ in both HClO₄ and NaOH at the used concentrations (data not shown). The remaining variable is R_{ct} . The fitting program determines that in HClO₄ R_{ct} is constant at $1 \Omega \text{ cm}^2$ over the whole potential range. However, these data could also be fitted assuming $R_{ct} = 0$, which does not noticeably change the accuracy of the fit. This shows that in fact R_{ct} in acidic media is too low to be measured accurately with our setup. In NaOH, however, R_{ct} increases from $30 \Omega \text{ cm}^2$ to $1 \text{ k}\Omega \text{ cm}^2$ in the H_{upd} potential range. In the double layer region R_{ct} decreases, after which it becomes comparable to acidic media in the OH potential region, and a value of $R_{ct} = 0 \Omega \text{ cm}^2$ would again give an equally satisfactory fit. These data suggest that the main difference between acidic and alkaline media is the difference in R_{ct} in the H_{upd} potential range.

Figure 10.6 shows a so-called frequency profile of the admittance spectra of Pt(111) in NaOH (10.6a) and HClO₄(10.6b). This frequency profile is constructed by plotting the real admittance at each potential and connecting the data points at

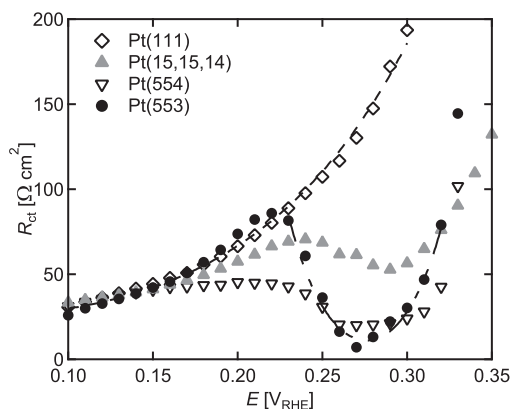


Figure 10.7 Charge transfer resistance (R_{ct}) as a function of potential for various Pt surfaces. An offset is used for Pt(553) and Pt(15,15,14). The dashed lines are fitted isotherms.

Surface	Offset [$\Omega \text{ cm}^2$]	R_{ct}^{\min} [$\Omega \text{ cm}^2$]	E_0 [V]	s	f	k [$\text{mol cm}^{-2} \text{ s}^{-1}$]
Pt(111)	–	34 ± 2	0.09 ± 0.009	0.51 ± 0.02	–3.8	1.6×10^{-8}
Pt(15,15,14)	+5	54 ± 1	0.28 ± 0.001	1.21 ± 0.09	0.6	2.8×10^{-7}
Pt(554)	–	19 ± 1	0.28 ± 0.001	1.79 ± 0.09	1.5	2.6×10^{-7}
Pt(553)	–30	13 ± 1	0.28 ± 0.001	1.85 ± 0.08	1.6	1.7×10^{-7}

Table 10.1 Fitted R_{ct} parameters. The rate constants are normalized for step density.

different potentials with the same frequency by a line. These are the lines in figure 10.6. The frequency profiles show that although the shapes of the admittance spectra are similar, the semi circle shifts to different frequencies at different potentials. In HClO_4 the top of the semi circle (1.1 mS) in the admittance plot in the H_{upd} potential region is at approximately 15 Hz. This shifts to ~ 150 Hz at 0.50 V and shifts back to ~ 15 Hz in the OH potential range. This is clearly due to the existence of C_{ad} in the H and OH adsorption regions. The NaOH frequency profile for admittance is comparable to that of HClO_4 except for the H_{upd} region. The values of the maxima of the two semi circles at 150 mV (0.4 and 1.5 mS) in this potential region are at ~ 5 and ~ 500 Hz, respectively. In this case, we also need to take into account R_{ct} in the H_{upd} region.

10.3.2 Stepped surfaces

For the stepped platinum single crystal surfaces we have performed the same equivalent circuit analysis as for Pt(111) with the circuit shown in figure 10.2. Since

we know from Pt(111) that only R_{ct} in the H_{upd} region in alkaline media is of interest, we show only R_{ct} for the different stepped Pt[$n(111) \times (110)$] surfaces (Pt(15, 15, 14), (554), and (553) with, respectively, $n = 29, 9,$ and 4) in NaOH from 0.10–0.35 V in figure 10.7, together with the R_{ct} of Pt(111) in this potential region. From 0.10–0.15 V the stepped Pt surfaces show the same trend in the R_{ct} as Pt(111), although the absolute resistance varied between different measurements. These differences in the R_{ct} of the stepped surfaces relative to Pt(111) could be due to some variation in the NaOH concentration. Since NaOH pellets are used there are small differences in the concentration between measurements which also cause small differences in the solution resistance R_s . This is reflected in the accuracy of the R_{ct} . Another reason for the difference could be different levels of contamination of the NaOH in the various measurements. For a better comparison between Pt(111) and the stepped Pt surfaces and to illustrate clearly the step density dependent trend in the R_{ct} , an offset to the fitted values (see table 10.1) for the R_{ct} curves of the stepped Pt surfaces is used such that they agree with the R_{ct} curve of Pt(111) between 0.10–0.15 V. This implies that the absolute magnitude of R_{ct} can be slightly different than shown here. We have taken several sets of data and verified that the well depth in the R_{ct} described next is independent of the absolute value of R_{ct} .

In the potential range between 0.22 and 0.35 V, the R_{ct} of the stepped surfaces decreases to a minimum at 0.28 V, after which it goes up again to the level of Pt(111). At this potential the current in the CVs of the stepped surfaces shows a peak as can be seen in the CVs of stepped surfaces in figure 11.1,^{180,181} which is assumed to be due to hydrogen adsorption at the steps. Therefore, the minimum in R_{ct} can be related to the charge transfer resistance at the steps.

The potential dependent R_{ct} data can be interpreted on the basis of a simple model for the adsorption processes following Langmuir or Frumkin statistics^{97,179,182}:

$$R_{ct} = R_{ct}^{\min} \cosh\left(\frac{1}{2}\bar{\phi}^*\right) \quad (10.2)$$

$$R_{ct}^{\min} = 2 \frac{RT}{n^2 F^2} [k_{ad} c_1 k_{des} c_2]^{-\frac{1}{2}} \quad (10.3)$$

$$\bar{\phi}^* = \bar{\phi} - f\left(\bar{\theta} - \frac{1}{2}\right) \quad (10.4)$$

$$\bar{\phi} = \frac{nF}{RT}(E - E_0) \quad (10.5)$$

with $\bar{\phi}^*$ the dimensionless potential, k_{ad} and k_{des} the rate constants for adsorption and desorption reactions, c_1 and c_2 the concentrations of the involved species, f the Frumkin parameter (which is zero under Langmuir conditions, negative for repulsive interactions and positive for attractive interactions), $\bar{\theta}$ the potential-dependent fractional surface coverage, E the potential, E_0 the potential for which $\theta = \frac{1}{2}$, $T = 298K$, n the number of electrons transferred in the reaction, and R and F have

their usual value.

Since it is well known that H_{upd} on Pt follows the Frumkin isotherm,^{99,183} *i.e.* $f \neq 0$, fitting equations (10.2–10.5) to the experimental data requires a cumbersome non-linear fitting procedure. However, the fitting procedure may be linearized by making use of the symmetry of the isotherm around $\bar{\theta} = \frac{1}{2}$. Since most of the fit will be done around $\theta = \frac{1}{2}$, we write a simple Taylor expansion:

$$\begin{aligned}\bar{\theta}(E) &= \frac{1}{2} + \left(\frac{d\theta}{dE}\right)_{\theta=\frac{1}{2}} (E - E_0) + \dots \\ &\approx \frac{1}{2} + \left(\frac{d\theta}{dE}\right)_{\theta=\frac{1}{2}} \frac{RT}{nF} \bar{\phi}\end{aligned}\quad (10.6)$$

where we ignore second-order terms from now on. The advantage of this procedure is that the dimensionless potential $\bar{\phi}^*$ is now a linear function of $\bar{\phi}$:

$$\bar{\phi}^* = s\bar{\phi}\quad (10.7)$$

with

$$s = 1 - \frac{RT}{nF} f \left(\frac{d\theta}{dE}\right)_{\theta=\frac{1}{2}}.\quad (10.8)$$

In other words, we have rescaled the potential by a factor s , related to the derivative of the isotherm at $\theta = \frac{1}{2}$, and this rescaling factor can be calculated from the various isotherm expressions.

For the two dimensional terraces $\left(\frac{d\theta}{dE}\right)$ is given by the Frumkin isotherm (see Appendix):

$$\left(\frac{d\theta}{dE}\right)_{\theta=\frac{1}{2}}^{\text{ter}} = -\frac{1}{4-f} \frac{F}{RT}\quad (10.9)$$

and for the one dimensional steps the exact solution is given by (see Appendix):

$$\left(\frac{d\theta}{dE}\right)_{\theta=\frac{1}{2}}^{\text{step}} = -\frac{e^{\frac{1}{2}f}}{4} \frac{F}{RT}.\quad (10.10)$$

Assuming the minimum in R_{ct} at ~ 0.28 V is due to the adsorption at the steps, equations (10.2) and (10.7) are fitted to the experimental R_{ct} data at Pt(111) (in the potential region 0.1–0.3 V) and the stepped Pt surfaces (in the potential region around 0.28 V) as shown by the dashed lines in figure 10.7. The resulting $R_{\text{ct}}^{\text{min}}$, s , and f are collected in table 10.1.

From these fit parameters the reference potential E_0 can be determined. This is also given in table 10.1. For Pt(111) E_0 is difficult to determine, since the lowest R_{ct} value for this surface lies at potentials lower than those measured in this data set, *i.e.* in the potential range where H_2 evolution starts. At the steps a value of 0.28 V

was found, which is the potential where R_{ct} goes through a minimum and the CV current exhibits a maximum.

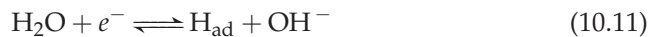
For Pt(111) we estimate a minimum adsorption resistance of $34 \Omega \text{ cm}^2$. Comparing to the stepped surfaces, R_{ct}^{min} is $13 \Omega \text{ cm}^2$ for Pt(553), the surface with the highest step density. Going to surfaces with a lower step density, R_{ct}^{min} increases to $54 \Omega \text{ cm}^2$ for Pt(15, 15, 14). This implies that R_{ct}^{min} decreases with increasing step density.

From R_{ct}^{min} also estimated values for the rate constant k for $E = E_0$ are calculated assuming that $k_{\text{ad}} = k_{\text{des}}$ (see table 10.1). For the H_{upd} at Pt(111) in 0.10 M NaOH we found a rate constant of $1.6 \times 10^{-8} \text{ mol cm}^{-2} \text{ s}^{-1}$. For the steps the rate constants are corrected for the various step densities and are found to be about one order of magnitude higher than on the terraces.

10.4 Discussion

The two semi circles in the admittance plots for Pt in alkaline media in the H_{upd} region indicate that two processes occur at different time scales. This can be explained by the equivalent circuit shown in figure 10.2: at high frequencies the impedances of both capacitors C_{dl} and C_{ad} are very low. The current, therefore, will go through the $R_s - -C_{\text{dl}}$ branch, to avoid R_{ct} . At lower frequencies the impedances of both capacitors are very high, but since $C_{\text{ad}} \gg C_{\text{dl}}$ all current will go through the $R_s - R_{ct} - C_{\text{ad}}$ branch. This difference can only be observed if R_{ct} is large enough compared to C_{dl} and C_{ad} . In the case of HClO_4 , R_{ct} is too low and, therefore, we cannot measure the value of R_{ct} or make a distinction between C_{dl} and C_{ad} . In this case the equivalent circuit reduces to a simple RC circuit. However, with a special setup, Sibert *et al.* measured impedance spectra in 0.5 M HClO_4 up to 1 MHz and estimated an R_{ct} value of $30.7 \text{ m}\Omega \text{ cm}^2$.¹⁷³ A second semicircle was observed at high frequencies. Note that this R_{ct} is indeed three orders of magnitude smaller than what we find in alkaline media.

A possible explanation for the significant difference in R_{ct} between acidic and alkaline media for the H_{upd} is that in basic solution it is expected that H transfers from water, whereas in acidic solution it transfers from H_3O^+ :



This would explain why the H_{upd} formation has a much higher resistance in alkaline media compared to acidic media if reaction (10.11) is slower than reaction (10.12). However, if we extrapolate this reasoning to the OH adsorption in HClO_4 , we would expect a high R_{ct} from 0.55–0.85 V, since OH in acidic media has to transfer from water via reactions similar to reaction (10.11). However, R_{ct} in the

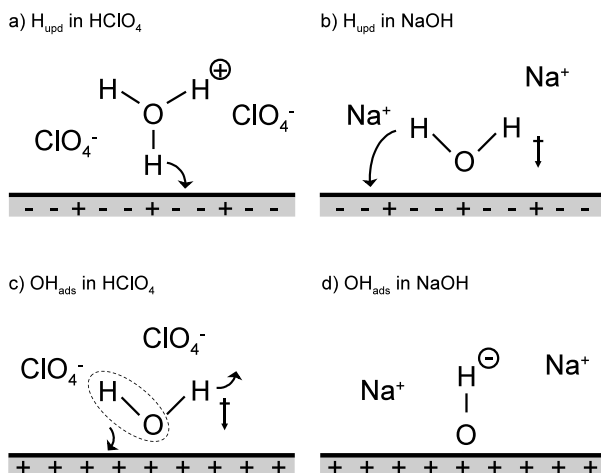


Figure 10.8 Suggested configurations at the interface for H_{upd} in (a) HClO_4 and (b) NaOH , and for OH^- adsorption in (c) HClO_4 and (d) NaOH .

OH^- region in acidic media is unmeasurably low. This cannot simply be explained by a difference in pH, since all measurements are referred to the RHE and therefore corrected for pH effects.

Numerous experimental studies, already since the beginning of the 20th century, show that the surface of water at a hydrophobic interface is negatively charged. This is explained by an abundance of OH^- ions at the surface (see ref. ¹⁸⁴ and references therein). This causes the surface of neat water to be basic.¹⁸⁵ Even though this conclusion has been debated in recent theoretical studies,^{186,187} a predisposition of the electrode/electrolyte interface towards an OH^- -abundant environment would explain why we do not observe a high R_{ct} in the OH^- adsorption region in acidic media. Ultra high vacuum studies show that the Pt(111) surface covered with one monolayer of H_2O is hydrophobic towards the adsorption of a second water layer,¹⁸⁸ providing us with a hydrophobic electrode/electrolyte interface. This could lead to a relative abundance of OH^- ions. Given that OH^- adsorption takes place in a potential region where the electrode is positively charged, such that all H^+ is expected to be expelled from the double layer, the local pH in the double layer may be such that OH^- ions may be available for adsorption on Pt, even in bulk acidic media.

Another explanation for the high R_{ct} in alkaline media is suggested in figure 10.8. Here, schematic drawings of the interface are shown for the H_{upd} (10.8a and 10.8b) and OH^- adsorption (10.8c and 10.8d) in acidic and alkaline media. This explanation focuses on a possible role of the electric field in the double layer on the orientation of the reactive species. For the H_{upd} in acidic media and the OH^- ad-

sorption in alkaline media (10.8a and 10.8d) it is obvious that in both cases the R_{ct} is very low, since the H_{upd} transfers directly from H_3O^+ , and OH^- adsorbs directly. In the two other cases, *i.e.* the H_{upd} in alkaline media and the OH^- adsorption in acidic media, one expects a higher R_{ct} , since they both have to transfer from water. However, the observed experimental difference might be related to the orientation of water at the interface. It is known that the orientation of water at the interface depends on the surface charge.^{189,190} In the H_{upd} potential range we expect the surface charge to be nearly neutral, possibly already becoming slightly positive, since it is assumed that the potential of zero total charge lies within this potential range.¹⁹¹ At higher potentials the surface charge is certainly positive. In the latter case, water at the interface is oriented with the oxygen towards the surface, thereby providing a facile transfer of OH^- as shown in figure 10.8c. However, in the case of alkaline media water is not expected to have a preferential orientation in the H_{upd} region, due to the lack of a high charge. Therefore, surface water may still have the orientation as shown in figure 10.8b, with the oxygen atom pointing towards the surface. This might explain why only in this particular case a high R_{ct} is measured, since the hydrogen of the water is pointing away from the surface, making its transfer to the surface a slow process.

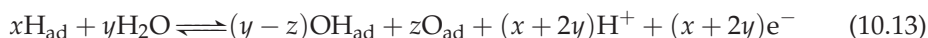
The R_{ct} data shown in figure 10.7 clearly illustrate a difference between terrace and steps on $Pt[n(111) \times (110)]$: the H_{upd} on Pt(111) leads to a broader R_{ct} curve compared to the H_{upd} on the steps. A narrower peak indicates attractive interactions between the hydrogen atoms at the steps. Therefore, the parameter s was introduced, which at step sites is approximately 1.8. For Pt(15,15,14) we obtained a lower value, but, since the step peak for this surface is less pronounced due to the low step density, we believe the values obtained at this surface are more prone to error. At the (111) terraces the value of s is lower than 1, indicating repulsive interactions between the adsorbed hydrogen atoms. From the parameter s the Frumkin parameter f is calculated using equations (10.9) and (10.10). The obtained Frumkin parameters are not the same as found by Oelgeklaus *et al.*, who found a Frumkin parameter of -13 for Pt(111), but the values are qualitatively similar. The quantitative difference may be related to a different OH^- concentration and to the different potential range over which the data are fitted to the theoretical isotherm. Since for Pt(111) the minimum in the R_{ct} lies outside of our measuring range, it is very difficult to determine its value accurately. The minimum adsorption resistance of $34 \Omega \text{ cm}^2$ found at the terraces is comparable to the value Oelgeklaus *et al.* found in a 0.1 M KOH solution for polycrystalline platinum,⁹⁷ even though there is a slight difference in pH and concentration. On the stepped surfaces we can determine E_0 , and therefore f , accurately.

The double layer capacitance we measured varies little between $10\text{--}30 \mu\text{F cm}^{-2}$, which is in good agreement with the values reported in literature. Using impedance and capacitance measurements, Pajkossy and Kolb obtained a value

of $\sim 20 \mu\text{F cm}^{-2}$.¹⁷⁴ Climent *et al.* used the CO displacement method and obtained similar C_{dl} values.¹⁹² With a thermodynamic approach, a C_{dl} of $14 \pm 5 \mu\text{F cm}^{-2}$ was calculated for the hydrogen adsorption region.¹⁹³

Our calculated rate constants are comparable to the values Oelgeklaus *et al.* obtained. They found for Pt(111) an adsorption rate of $6.5 \times 10^{-8} \text{ mol cm}^{-2} \text{ s}^{-1}$. It is already known that at steps the H_{upd} is faster compared to the terraces of Pt single crystal surfaces.

Koper *et al.* compared CVs of Pt(111) and stepped Pt surfaces in sulfuric acid and modeled the CVs with Monte Carlo simulations.¹⁰² In order to fit the CVs a lateral interaction energy of 4.5 kJ mol^{-1} (repulsive) was used for the (111) terraces, versus an interaction energy of -20 kJ mol^{-1} (attractive) for the steps. The interaction energies derived from the CV fitting in acidic media correspond to Frumkin parameters of $f \approx -11$ and $f \approx +8$, respectively, *i.e.* both the repulsive and attractive interactions appear stronger in acidic media than what we find in alkaline media. It is well-known that the interaction between adsorbed hydrogens on Pt(111) is weak but repulsive.^{59,165} The attractive interactions on the steps are more difficult to explain. The competitive adsorption of hydrogen and bromide is known to cause a sharp peak in the CV, which is ascribed to effective attractive interactions, resulting from the fact that the repulsive H–Br interactions exceed the sum of the H–H and Br–Br repulsive interactions.¹⁹⁴ The effective attractive lateral interactions found in the steps can be likewise explained, if we assume that the sharp peak at 0.28 V in both the CV and the R_{ct} curve is caused by competitive co-adsorption. A possible candidate for a co-adsorbing species is OH. However, chapters 4–6 suggest that when water is co-adsorbed with O on a stepped Pt surface, OH_{ad} on the steps is not very stable and atomic O remains present. Therefore, we propose



as the reaction, in which H_{ad} is replaced by OH_{ad} and/or O_{ad} . This reaction would also explain why only a single peak is observed for the steps, whereas on the Pt(111) terraces the H and OH adsorption are separated. Note that this explanation is not very different from the usual assumption that on Pt(100) and Pt(110), there is no double layer region, but the H_{upd} region is immediately followed by the OH_{ad} region.¹⁹⁵ What we suggest here, is that the same applies for steps of that orientation. The detailed consequences of this model will be discussed in chapter 11.

10.5 Conclusions

We have shown here using impedance spectroscopy that, in spite of the similar looking CVs, the H_{upd} in acidic and alkaline media shows a significant difference. The R_{ct} in alkaline media is on the order of $1 \text{ k}\Omega \text{ cm}^2$, whereas in acidic media it was

too low to be measured with our set-up. We do not find a difference in the R_{ct} for the OH adsorption. Tentatively, this is explained by the relative abundance of OH^- at the interface, or by the orientation of water at the interface which could make the transfer of hydrogen slower in alkaline media. The charge transfer resistances obtained in alkaline media are fitted with theoretical isotherms. At the terrace we find repulsive lateral interactions between hydrogen atoms, whereas at the steps the interactions are attractive. We explain the effective attractive interactions by a competitive replacement reaction at the steps.

